From field to office — A fast-track beam depth migration with tomography updates applied to blended data

Ali Alzayer[1], Constantine Tsingas[1], Nick Tanushev[2], Mihai Popovici[2], and Mohammed Almubarak[1]

https://doi.org/10.1190/tle44080614.1

Abstract

A new mode of imaging "fast-track" operations has been developed in which field blended data are processed through a fast beam migration with tomography updates to obtain an efficient and reliable depth imaging result while the crew is still in the field. Over the past several years, empirical studies utilizing broadband seismic data recording, processing, and interpretation have consistently demonstrated significant improvements in subsurface imaging and characterization, as evidenced by numerous case studies. Significant research has focused on optimizing the emission, recording, and processing of both low- and high-frequency seismic data to enhance image reliability. Recent advancements in seismic source and receiver technology, coupled with the implementation of blended acquisition field configurations, have enabled geoscientists to achieve more efficient data acquisition and capture wider frequency bandwidths. A unique aspect of this research is the combined application of an efficient acquisition strategy and the accelerated, fast-track, imaging of blended data. This enables the creation of velocity-depth models and associated depth images without relying on complex inversion deblending techniques. We first present a targeted seismic acquisition methodology, crafted for the efficient and optimal recording of broadband data via a dispersed source array. Subsequently, we present the results of our investigation into the technologies employed, demonstrating their capability to deliver fast-track depth images and associated velocity-depth models during blended acquisition field operations.

Introduction

Effective seismic acquisition surveys are typically designed to optimize three key parameters: (1) achieving high spatial density in source and receiver locations to maximize subsurface illumination and wavefield sampling, (2) ensuring comprehensive broadband frequency coverage, and (3) maintaining cost-efficiency throughout the acquisition process. In recent years, blended seismic acquisition has enhanced field productivity by enabling simultaneous source activations, thereby increasing data acquisition speed and reducing overall survey time. Earlier work on blended acquisition used the independent simultaneous sweeping method, a technique that allows for increased vibroseis productivity and sampling density by treating interference from multiple unsynchronized sources as noise, with a focus on contrasting its performance against other advanced vibroseis methods and exploring the impact of different sweep types (Howe et al., 2008). Berkhout (2012) proposed "inhomogeneous blending" for seismic source arrays, utilizing dispersed narrowband sources with optimized parameters for different frequency ranges, to improve efficiency and enable robotic acquisition, contrasting with traditional "homogeneous blending" of identical broadband sources.

This research aimed to evaluate the integrated workflow of unconstrained blended seismic data acquisition and concurrent field-based data processing. The objective was to determine the feasibility of utilizing real-time insights from "fast-track" depth processing, such as data quality assessment or illumination analysis, to provide actionable feedback to the acquisition crew for immediate, adaptive decision-making. In addition, the obtained depth images can be considered as a "first look" by the interpreters. The integration of beam migration with automated tomographic velocity updates presents a velocity model building methodology that significantly reduces turnaround time compared to conventional reflection tomography while preserving velocity model accuracy. The capability of this method for real-time processing is exemplified by the generation of a preliminary depth stack and associated velocity-depth model from 3D blended seismic data during ongoing field operations.

As part of an effort to reduce the acquisition cycle time, increase productivity, and improve seismic imaging and resolution while optimizing costs, a novel seismic acquisition survey was conducted employing 24 vibrators generating two different types of sweeps in a 3D unconstrained, decentralized, and dispersed source array (DSA) field configuration inspired by works of Berkhout (2012). The blended acquisition design achieved a maximum of 65,000 vibrator points during 24 hours of continuous recording window, demonstrating significantly higher field productivity compared to the conventional seismic survey operated in the same area using a nonblended centralized source mode. After applying different deblending algorithms, depth-migrated images were obtained. In addition, two data sets (i.e., low and medium-high frequency sources) were integrated to obtain full-bandwidth broadband seismic images. Comparative analysis between the distributed and unconstrained blended and nonblended conventional seismic surveys — acquired by the same crew during the same time over the same area — revealed high similarity between the two data sets (Tsingas et al., 2020).

An integrated approach, utilizing fast beam migration (FBM) for accelerated beam-based depth imaging and automated tomographic updates, was employed to enhance the efficiency of velocity-depth model generation for subsurface imaging. The land

Manuscript received 9 November 2024; revision received 20 March 2025; accepted 14 April 2025.

[1]Saudi Aramco, EXPEC Advanced Research Center, Dhahran, Saudi Arabia. E-mail: ali.alzayer.1@aramco.com, constantinos.tsingas@aramco.com; mohammed.mubarak.6@aramco.com.

[2]Z Terra Inc., Houston, Texas, USA. E-mail: nicktan@z-terra.com; mihai@z-terra.com.

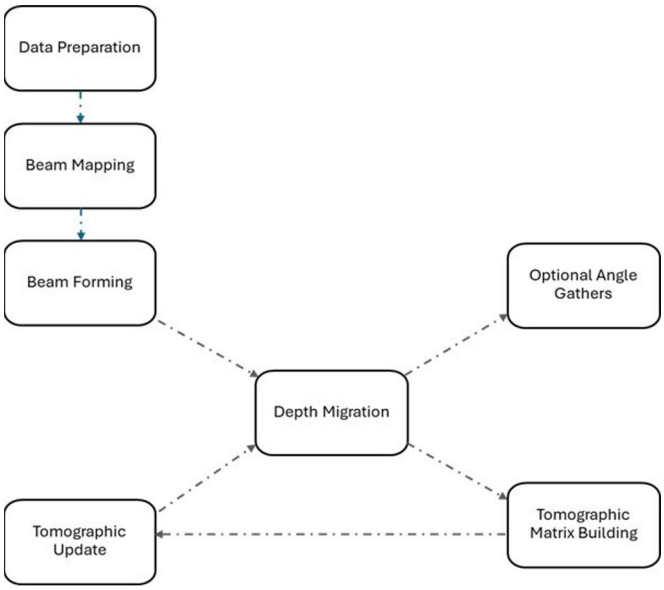

Figure 1. Graph shows the FBM with tomography workflow from data preparation until the final velocity model update. For each velocity model update, depth migration, tomography matrix building, and tomographic inversion are performed automatically to align the migrated beams. Optionally, angle gathers can be generated at certain iterations for QC.

seismic data used in this paper were acquired using field acquisition configurations based on a variation of the DSA concept (Berkhout, 2012; Tsingas et al., 2016). Compared to standard Kirchhoff depth migration algorithms, FBM offers significantly enhanced computational speed and facilitates multipath imaging, effectively accommodating abrupt lateral velocity variations, a characteristic typically associated with wave-equation migration algorithms.

This paper presents a successful application of FBM with tomography updates on raw recorded field data (i.e., blended) and compares the results obtained with the corresponding deblended seismic data.

Method

Beam tomography is an automated approach that combines FBM with an optimized beam-domain reflection tomography. Beam-based techniques were studied at length in literature where it has been demonstrated that the accuracy of beam-based methods is generally controlled by the beam forming parameters (Červený et al., 1982; Weber, 1988; Hill, 2001). During FBM, the traces of the input data are subdivided and transformed into beams representing locally coherent events characterized by an arrival time, wavelet signature, source and receiver locations, dip orientation, and curvature (Fomel and Tanushev, 2009). As a result, the subsequent depth migration is faster than conventional Kirchhoff-based migration techniques where each individual trace is migrated. Beam-domain reflection tomography uses an automated methodology to estimate residual moveout and thus is making the velocity model updates significantly faster than conventional reflection tomography. If the image generated by a beam pair is not in agreement with the image produced by other beams, a shift is needed in the direction perpendicular to the reflector that the beam is imaging. Converting those depth shifts into local velocity perturbations allows us to build an azimuthally dependent tomographic solution (Sherwood et al., 2011; Tanushev et al., 2017).

A typical beam migration workflow consists of beam mapping, beam forming, depth migration, and image forming. In beam mapping, data are subdivided into smaller blocks with limited offsets according to the desired geometry of estimated beams. Several techniques such as local plane wave destructive filter and local slant stack can be used in the beam forming stage. The beam forming stage represents a major computational cost in the FBM workflow; however, it only needs to be done once because the beam events are independent of the velocity model.

Beam tomography combines aspects of beam migration and automated tomography to iteratively create computationally efficient velocity depth models. Figure 1 shows the automated (FBM) tomography workflow used in the velocity model building process. In this study, FBM with tomography updates was applied to both a blended seismic data set and the deblended version of the acquired survey to achieve reliable velocity models. We show that applying FBM tomography to blended data will produce very similar results as with properly deblended data.

Results

The 3D seismic data were acquired using the field concept of DSA where several unconstrained and decentralized sources operate in a blended acquisition design (Berkhout, 2012; Tsingas et al., 2020). Multiple sources were triggered simultaneously, resulting in the collection of a high-density broadband blended data. The blended acquisition mode significantly shortened the operational time in the field, but it generated a significant amount of crosstalk noise. Deblending techniques, employing sparse inversion methodologies, can effectively suppress crosstalk noise. Tsingas et al. (2020) presented full details on the processing workflow using novel techniques to deblend the data in this specific example. In terms of fast turnaround time, the following indicative field productivity metrics were achieved: for a partial block of acquisition 100 km^2, using 38,000 recording channels, 24 vibrators were utilized, producing an average of 50,000 sweeps per 24-hour day of operations and a duration of three days recording 30 million traces per square kilometer. Moreover, it took three days for fast-track processing, including FBM tomography producing image gathers, of this partial volume using 200 CPU nodes (dual 20 cores, 384 GB RAM per node). Therefore, in six days we have acquired and processed 100 km^2 generating a multiplicity of velocity-depth models and their corresponding depth images and associated image gathers while the seismic crew was still acquiring data in the vicinity (Tsingas et al., 2020).

Figure 2 shows seismic common receiver gathers before and after deblending. The blending noise in blended shot gather data exhibits coherent events, whereas in any other data domain (i.e., common receiver, common midpoint, and common offset) it appears incoherent and is regarded as an outlier or noise interference or crosstalk. The incoherent characteristics of the crosstalk noise is the discriminating factor, which was used during the sparse inversion in the deblending process.

The challenge is to produce a meaningful depth stack using the field data directly. For comparison, three months in the

processing shop were needed to produce results using the processed deblended data. A typical deblending process aims to differentiate between overlapping energy sources and produce subsequent seismic gathers for processing. The beam tomography workflow in Figure 1 was executed to both the field (blended) and processed (deblended) data to examine the robustness of the FBM tomography application even in the presence of crosstalk noise. Figure 3 and Figure 4 show a portion of the data with beam estimation computed from blended and deblended data sets, respectively, generated from a set of source and receiver beam pairs. The estimated beams will be further migrated using an initial velocity depth model to create common image angle gathers as an input for tomography updates.

About 20 iterations were required for both data sets, i.e., blended and unblended, to produce flat FBM angle gathers, which are depicted in Figures 5 and 6, respectively. Common image angle gathers after migration and several velocity depth model updates exhibit flat events, demonstrating a convergence to an acceptable solution. Illumination issues are expected at the edges of the seismic survey for both data sets due to low acquisition fold and differing noise characteristics between source and receiver beams. Beam forming relies heavily on the fact that seismic events are locally linear in the source and receiver coordinates. In other words, moving the source x coordinate a certain amount will result in a temporal shift in the recorded wavelet, and moving the source x coordinate twice as far will result in twice the temporal shift. The same holds true for the source y and receiver x and y coordinates. The goal of beam forming is to detect the linear relationship between the trace coordinates and the temporal shift as a four-dimensional dip. This characteristic is a primary factor leveraged by FBM algorithms in the context of blended seismic data processing. For the crosstalk shot to appear linear in the source coordinates, the second source must match the cadence and relative motion of the first source. This is rather unlikely to be true for all the traces that are used for beam forming (see Figure 3 for a "bundle" of traces used for beam forming). This is the first place that the crosstalk is eliminated. In addition, crosstalk, even when identified as a linear event by beam forming, will likely be eliminated as an erroneous event during the imaging and migration stages. The estimated dips from beam forming are used as the initial ray tracing direction from the source and receiver locations. For migration to place the event in the subsurface, these two rays have to meet (or nearly meet) and the traveltime along those two rays must be equal to the recording time of the seismic event. This is also unlikely to happen because the primary and secondary sources are situated a relatively large distance apart, as is common practice in blended acquisitions. Therefore, the crosstalk is naturally eliminated during the FBM workflow. Subsurface reflectivity images were retrieved through a successful application of the FBM tomography on the blended and deblended data sets. Notably, comparable velocity models were obtained using FBM for both data sets and are depicted in Figure 7. The results highlight the effectiveness of FBM tomography even when blended data are used as input to the process.

To evaluate the tomographic updates, we computed a beam illumination volume shown in Figure 8. The beam illumination quantitatively measures how many beams through depth migration have visited the same subsurface point. These sets of beams are used to create the tomography matrix and further update the

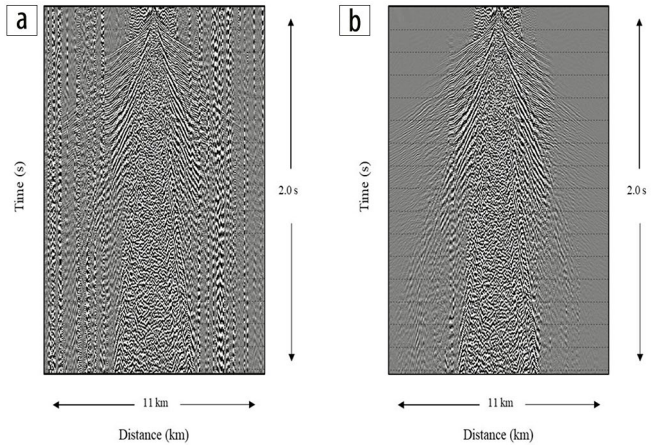

Figure 2. (a) A blended 3D receiver gather in which the associated crosstalk noise (vertical stripes) is stronger than actual reflections. (b) The corresponding deblended receiver gather where most of the blended noise has been eliminated.

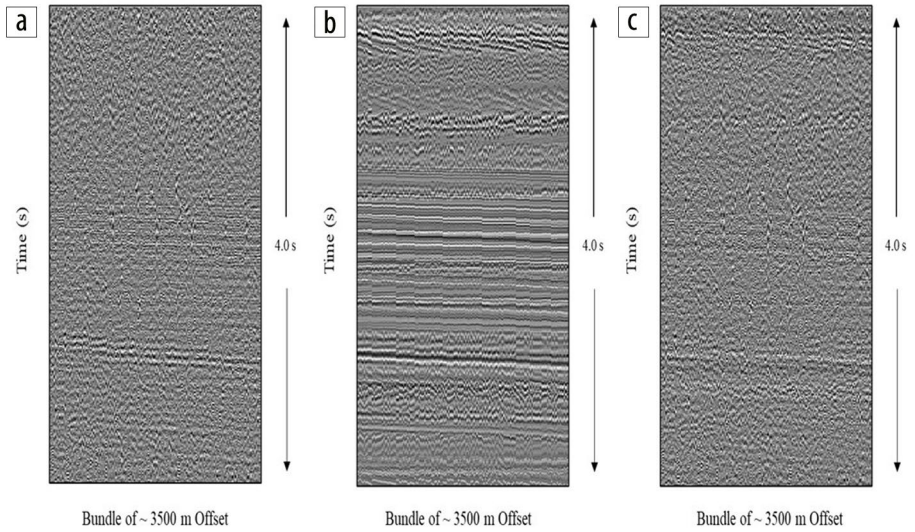

Figure 3. Illustration of the beam forming or locally coherent events selection from blended data of a random shot and receiver beam pairs separated by 3500 m offset. This bundle is the collection of traces that is used for beam forming. The traces in a bundle have their source and receiver coordinates within a short distance of a central source and receiver coordinate pair. Note that this implies that the common midpoint coordinates of these traces are also within a small distance of each other and the offsets are also within a small range. (a) Input blended data. (b) The estimated beams to be depth migrated and used in the tomography workflow. (c) The residual noise between the original input data in (a) and the estimated beams in (b). The traces in each panel are sorted by offset.

velocity model through an LSQR solver. In general, the deblended data show higher beam intensity than blended data. This could be due to some residual noise accompanying migrated beams during their imaging. In addition, no significant updates were made on the deeper section (< 2.5 km) due to illumination limitations and lack of far offset data (up to 6 km). Areas above the black boundary highlight superior illumination and provide confidence in the tomography updates for both velocity models. Other factors control the illumination, including the acquisition design, which suggests that longer offsets are necessary to image the deeper section and short offsets to be able to image the shallow part. However, the most significant aspect of this entire exercise is the time required to generate both migrated stacks.

Conclusion

As part of reducing the acquisition cycle time in the seismic value chain and improving seismic broadband imaging and resolution while optimizing costs, a novel acquisition survey was conducted and an efficient workflow was followed in order to obtain reliable "real time" depth images. This blended survey was based on the DSA concept employing 24 vibrators generating two different types of sweeps operating in a 3D unconstrained and decentralized field configuration mode. A novel workflow was applied to the field blended data consisting of FBM combined with "hands free" tomography updates. Similar depth imaging results were obtained by applying the same workflow on the deblended version of the data, which proves the concept and the robustness of "first look or fast-track depth imaging" using field blended data. Consequently, the benefits of acquiring ultra-high trace density data using a decentralized and unconstrained source blended mode produced high-quality broadband seismic images in significantly shorter turnaround time and without sacrificing data quality. Furthermore, the application of FBM with tomography updates on both data sets, i.e., blended and deblended, succeeded in achieving comparable velocity model updates. Therefore, future field applications of the methodology can follow up the acquisition crew and produce in almost "real time" accurate depth images that can possibly provide acquisition alternative design scenarios. The ultra-fast nature of FBM with tomography updates may also reduce

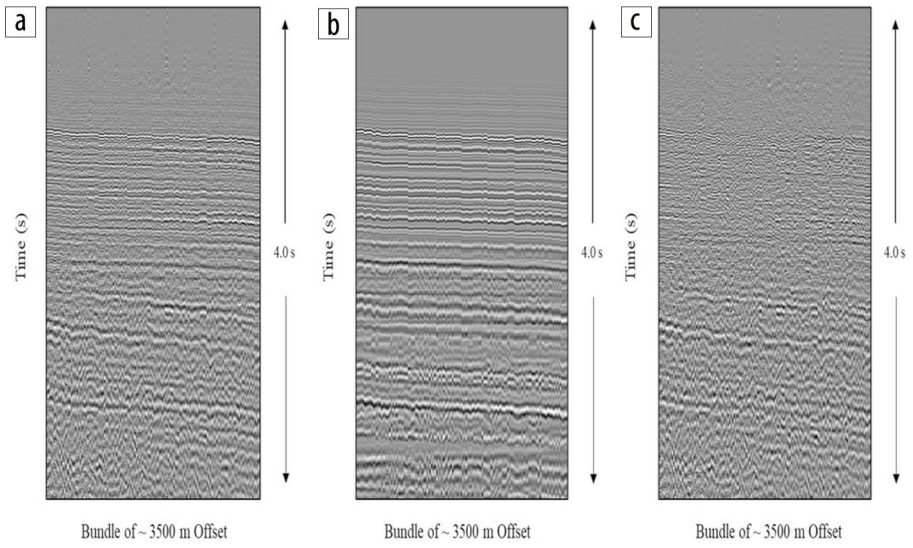

Figure 4. An illustration of the beam forming or locally coherent events selection from the deblended data of a random shot and receiver beam pairs separated by 3500 m offset. The previous figure contains a brief explanation of the shown bundles. (a) Input deblended data (cleaner than those shown in Figure 3a). (b) The estimated beams to be depth migrated and used in the tomography workflow. (c) The residual noise between the original input data in (a) and the estimated beams in (b).

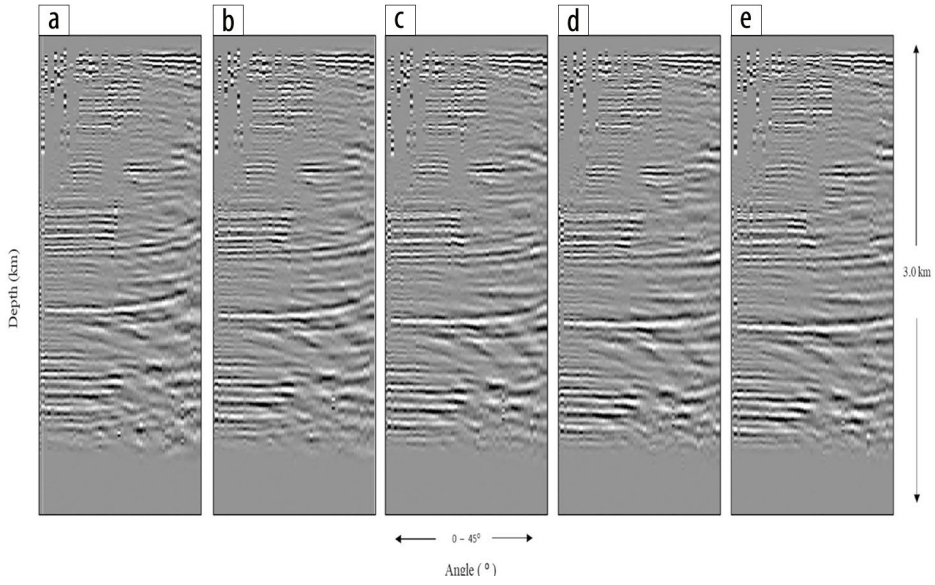

Figure 5. (a) An illustration of common image angle gathers from the blended (DSA) data after (a) first iteration, (b) fifth iteration, (c) 10th iteration, (d) 15th iteration, and (e) 20th iteration of FBM with tomography updates. There is still some residual moveout at later arrivals where anisotropy was not accounted for due to fast-track processing.

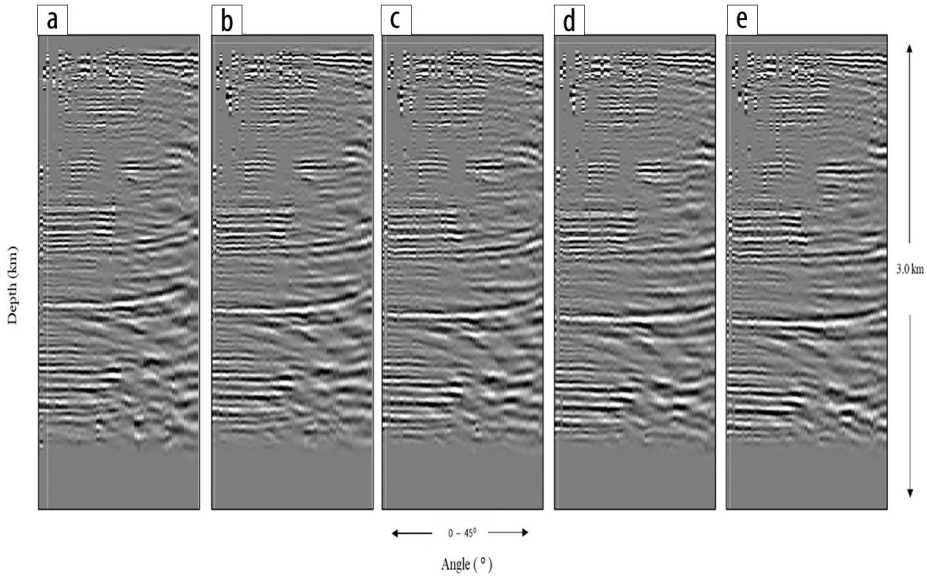

Figure 6. An illustration of common image angle gathers from the deblended data after (a) first iteration, (b) fifth iteration, (c) 10th iteration, (d) 15th iteration, and (e) 20th iteration of FBM with tomography. There is still some residual moveout at later arrivals where anisotropy was not accounted for due to fast-track processing.

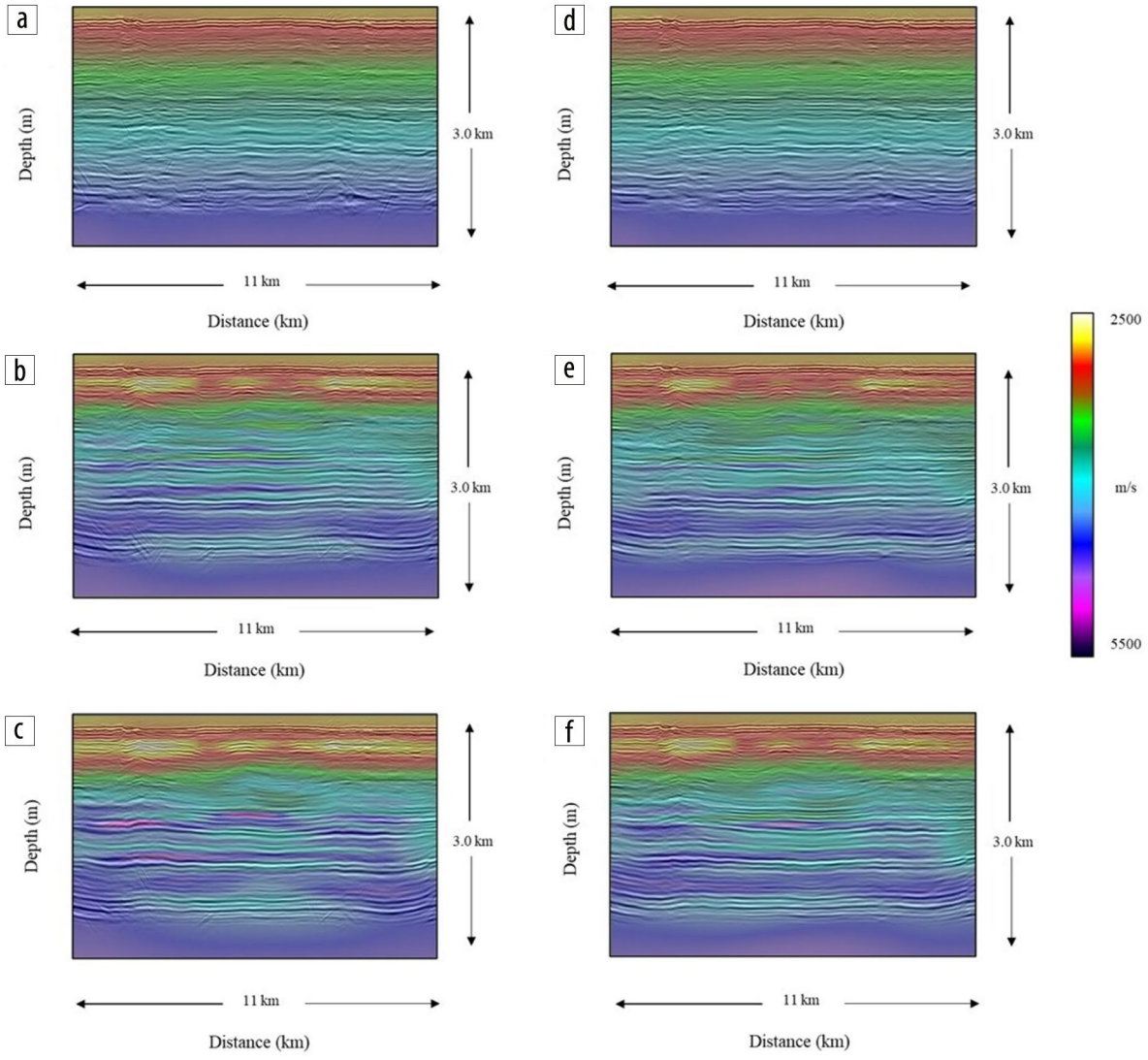

Figure 7. An illustration of the velocity model update from blended data on left panels after (a) first iteration, (b) 12th iteration, and (c) 21st iteration. The right panels show the velocity model update from the deblended data after (d) first iteration, (e) 12th iteration, and (f) 21st iteration of FBM with tomography. A reflectivity image overlays each velocity model update to correlate imaged events and background velocity model.

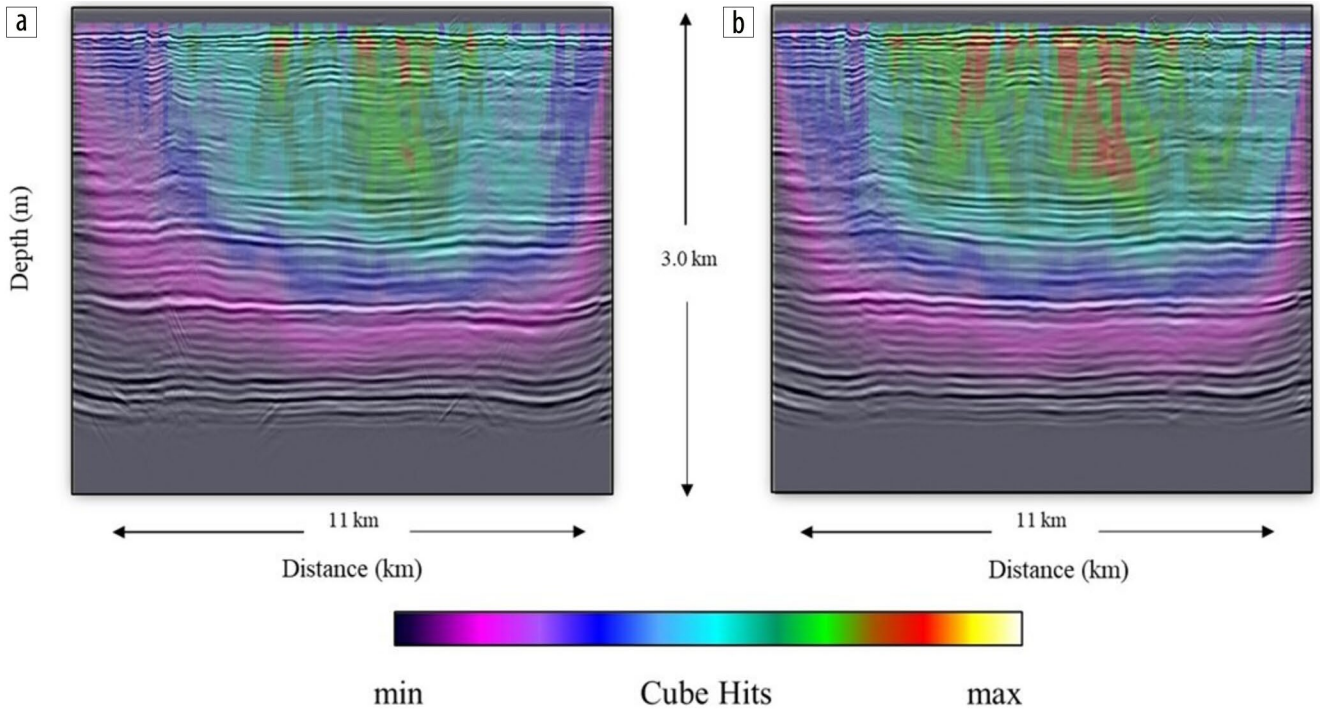

Figure 8. An illustration of beam illumination achieved after depth migration, overlayed by its respective reflectivity image, using the final the velocity model update from (a) blended and (b) deblended data after 21 iterations of FBM tomography. Note that warm colors indicate higher beam illumination in the subsurface.

iterations during full-waveform inversion and least-squares reverse time migration applications and contribute as a real-time solution for seismic monitoring of CO_2 sequestration projects through accelerated imaging. TLE

Data and material availability

Data associated with this research are confidential and cannot be released.

Corresponding author: ali.alzayer.1@aramco.com

References

Berkhout, A. J., 2012, Blended acquisition with dispersed source arrays: Geophysics, **77**, no. 4, A19–A23, https://doi.org/10.1190/geo2011-0480.1.

Červený, V., M. M. Popov, and I. Pšenčík, 1982, Computation of wave fields in inhomogeneous media — Gaussian beam approach: Geophysical Journal International, **70**, no. 1, 109–128, https://doi.org/10.1111/j.1365-246X.1982.tb06394.x.

Fomel, S., and N. Tanushev, 2009, Time-domain seismic imaging using beams: 79th Annual International Meeting, SEG, Expanded Abstracts, 2747–2752, https://doi.org/10.1190/1.3255419.

Hill, N. R., 2001, Prestack gaussian-beam depth migration: Geophysics, **66**, no. 4, 1240–1250, https://doi.org/10.1190/1.1487071.

Howe, D., M. Foster, T. Allen, B. Taylor, and I. Jack, 2008, Independent simultaneous sweeping — A method to increase the productivity of land seismic crews: 78th Annual International Meeting, SEG, Expanded Abstracts, 2826–2830, https://doi.org/10.1190/1.3063932.

Sherwood, J., J. Jiao, H. Tieman, K. Sherwood, C. Zhou, S. Lin, and S. Brandsberg-Dahl, 2011, Hybrid tomography based on beam migration: 81st Annual International Meeting, SEG, Expanded Abstracts, 3979–3983, https://doi.org/10.1190/1.3628037.

Tanushev, N., A. M. Popovici, and S. Hardesty, 2017, Fast, high-resolution beam tomography and velocity-model building: The Leading Edge, **36**, no. 2, 140–145, https://doi.org/10.1190/tle36020140.1.

Tsingas, C., M. Almubarak, W. Jeong, A. Al Shuhail, and Z. Trzesniowski, 2020, 3D distributed and dispersed source array acquisition and data processing: The Leading Edge, **39**, no. 6, 392–400, https://doi.org/10.1190/tle39060392.1.

Tsingas, C., Y. Kim, and J. Yoo, 2016, Broadband acquisition, deblending, and imaging employing dispersed source arrays: The Leading Edge, **35**, no. 4, 354–360, https://doi.org/10.1190/tle35040354.1.

Weber, M., 1988, Computation of body-wave seismograms in absorbing 2-D media using the gaussian beam method: comparison with extract method: Geophysical Journal International, **92**, no. 1, 9–24, https://doi.org/10.1111/j.1365-246X.1988.tb01116.x.